



OPEN ACCESS

EDITED BY

Nazia Manzar,
National Bureau of Agriculturally Important
Microorganisms (ICAR), India

REVIEWED BY

Jinyun Li,
University of Florida, United States
Hemant S. Maheshwari,
ICAR Indian Institute of Soybean Research,
India
Divya Joshi,
G. B. Pant University of Agriculture and
Technology, India

*CORRESPONDENCE

Jeri D. Barak
✉ barak@plantpath.wisc.edu

RECEIVED 16 December 2024

ACCEPTED 21 January 2025

PUBLISHED 03 February 2025

CITATION

Cowles KN, Iyer AS, McConnell I,
Guillemette EG, Nellore D, Zaacks SC and
Barak JD (2025) Established *Pseudomonas*
syringae pv. *tomato* infection disrupts
immigration of leaf surface bacteria to the
apoplast.
Front. Microbiol. 16:1546411.
doi: 10.3389/fmicb.2025.1546411

COPYRIGHT

© 2025 Cowles, Iyer, McConnell, Guillemette,
Nellore, Zaacks and Barak. This is an
open-access article distributed under the
terms of the [Creative Commons Attribution
License \(CC BY\)](https://creativecommons.org/licenses/by/4.0/). The use, distribution or
reproduction in other forums is permitted,
provided the original author(s) and the
copyright owner(s) are credited and that the
original publication in this journal is cited, in
accordance with accepted academic
practice. No use, distribution or reproduction
is permitted which does not comply with
these terms.

Established *Pseudomonas syringae* pv. *tomato* infection disrupts immigration of leaf surface bacteria to the apoplast

Kimberly N. Cowles¹, Arjun S. Iyer², Iain McConnell²,
Ellie G. Guillemette¹, Dharshita Nellore¹, Sonia C. Zaacks¹ and
Jeri D. Barak^{1*}

¹Department of Plant Pathology, University of Wisconsin-Madison, Madison, WI, United States, ²Data Science Institute, University of Wisconsin-Madison, Madison, WI, United States

Bacterial disease alters the infection court creating new niches. The apoplast is an oasis from the hardships of the leaf surface and is generally inaccessible to nonpathogenic members of the phyllosphere bacterial community. Previously, we demonstrated that *Salmonella enterica* serovar Typhimurium (*S. Typhimurium*) immigrants to the leaf surface can both enter the apoplast and replicate due to conditions created by an established *Xanthomonas hortorum* pv. *gardneri* (Xhg) infection in tomato. Here, we have expanded our investigation of how infection changes the host by examining the effects of another water-soaking pathogen, *Pseudomonas syringae* pv. *tomato* (Pst), on immigrating bacteria. We discovered that, despite causing macroscopically similar symptoms as Xhg, Pst infection disrupts *S. Typhimurium* colonization of the apoplast. To determine if these effects were broadly applicable to phyllosphere bacteria, we examined the fates of immigrant Xhg and Pst arriving on an infected leaf. We found that this effect is not specific to *S. Typhimurium*, but that immigrating Xhg or Pst also struggled to fully join the infecting Pst population established in the apoplast. To identify the mechanisms underlying these results, we quantified macroscopic infection symptoms, examined stomata as a pinch point of bacterial entry, and characterized aspects of interbacterial competition. While it may be considered common knowledge that hosts are fundamentally altered following infection, the mechanisms that drive these changes remain poorly understood. Here, we investigated these pathogens to reach a deeper understanding of how infection alters a host from a rarely accessible, inhabitable environment to an obtainable, habitable niche.

KEYWORDS

plant microbe interaction, food safety, *Salmonella enterica*, niche adaptation, plant pathogen

Introduction

Hosts become a fundamentally altered niche following infection. Any plant pathology textbook offers many examples of how pathogens can modify the morphology of hosts with the level of modification ranging from intracellular to the whole organism (Agrios, 2005). While these changes are well-documented, it remains unknown how changes to the host create new and preferred niches for organisms beyond the infecting pathogen. We and others have demonstrated that infected plants increase the incidence of rare members of the plant microbiota, namely bacterial human pathogens, such as *Salmonella enterica* (Cowles et al., 2022; Dixon et al., 2022; Potnis et al., 2014, 2015; Barak et al., 2008; Kwan et al., 2013; Wells

and Butterfield, 1997; Yang et al., 2020; Ginnan et al., 2020; Gao et al., 2021). This increase in incidence and population growth results from the conversion of the rarely accessible, inhabitable interior space of the leaf, the apoplast, to an obtainable, habitable niche following infection.

Epiphytic bacteria, those found on the surface of plants, tolerate a harsh environment with rapidly fluctuating conditions. Survival of recent bacterial immigrants on a leaf surface is mostly due to luck on arrival near or in an oasis of nutrient and water availability, the base of glandular trichomes or in the grooves between cells (Monier and Lindow, 2003, 2004; Barak et al., 2011). Flagellar motility and the capacity to form aggregates, either inter- or intra-species, increases an immigrant's probability of survival (Haefele and Lindow, 1987; Lindow et al., 1993). Success requires adaptation to changes in water or nutrient availability, temperature, and UV irradiation levels, among others. Bacterial phytopathogens lacking cell wall degrading enzymes abandon the leaf surface and choose the apoplast for their infection court. The leaf apoplast has several obvious advantages over the leaf surface: protection from most UV irradiation, little to no cuticular wax encasing plant cell surfaces, and reduced fluctuation in free water. Although the existence of bacteria in the apoplast is well documented by microscopy (Boureau et al., 2002), along with many bacterial factors that are necessary for disease, in general, little is known about the dynamic colonization of an infected apoplast during disease progression and distinct changes in the infected host.

One of most widely studied bacterial-plant interactions is *Arabidopsis thaliana* as a model host for *Pseudomonas syringae* pv. *tomato* (Pst). Pst uses a jasmonic acid mimic coronatine (COR) to open stomata for access to the leaf apoplast (Melotto et al., 2006). Pst then further manipulates the host immune system using Type III effectors HopM1 and AvrE to induce the abscisic acid pathway and to close stomata to increase water potential in the apoplast (Melotto et al., 2017; Roussin-Léveillé et al., 2022; Hu et al., 2022). These findings are the foundational understanding of the disease Pst causes in tomato, bacterial speck. A macroscopically similar disease, bacterial spot of tomato, is caused by four lineages of *Xanthomonas*: *X. hortorum* pv. *gardneri* (hereafter referred to as Xhg), *X. euvesicatoria* pv. *euvesicatoria*, *X. euvesicatoria* pv. *perforans*, and *X. vesicatoria* (Jones et al., 1998; Osdaghi et al., 2021; Timilsina et al., 2020). Tomato infection with either Pst or Xhg is characterized by water-soaked lesions and abundant phyto-bacterial growth.

Multiple works from our lab have demonstrated that Xhg infection alters the tomato host in ways that benefit non-phytopathogenic bacteria inhabiting the leaf surface (Cowles et al., 2022; Dixon et al., 2022; Potnis et al., 2014, 2015). Although the primary purpose of altering the plant environment during infection is likely for the benefit of the pathogen, sweeping changes in physical and biochemical characteristics of the host reshape the composition of the bacterial community in an infection court as shown in both human (Manos, 2022) and plant infections (Griffiths et al., 2020; Hu et al., 2020). Bacterial communities in multiple plant systems are impacted by the changes that occur during disease progression (Gao et al., 2021; Li et al., 2022; Huang et al., 2023). In tomato, we have found that the dramatic change to the apoplast as a result of Xhg infection creates an available and habitable niche for bacteria that are usually precluded from stomatal entry and exiled to the leaf surface, such as *S. enterica* serovar Typhimurium (*S. Typhimurium*) (Cowles et al., 2022; Dixon et al., 2022; Potnis et al., 2014, 2015). Xhg infection does two things: (1) permits *S. Typhimurium* access to the apoplast, a niche that the

human pathogen cannot access on its own and (2) transforms the apoplast into a habitable niche for *S. Typhimurium*, altering the apoplast in ways that promote bacterial replication (Cowles et al., 2022; Dixon et al., 2022; Potnis et al., 2014, 2015). However, the mechanisms driving changes to the host that create new and preferred niches for organisms beyond the infecting pathogen and that influence bacterial dynamics in the apoplast remain unknown.

Here, we expanded our investigation of how leaf infection impacts the host and examined whether bacteria that create a water-soaked apoplast during infection, in general, permit leaf surface bacteria entry to this altered niche. We discovered that, unlike Xhg infection which promotes *S. Typhimurium* success, Pst infection disrupts *S. Typhimurium* colonization of the apoplast. In addition, we found that this effect is not specific to *S. Typhimurium*, but that immigrating populations of Xhg or Pst also struggled to join the infecting Pst population established in the apoplast. These results support several possible mechanisms that we began to investigate in this work: (1) changes to a Pst-infected plant result in a barrier to apoplast entry, (2) Pst infection creates an inhospitable niche, or (3) macroscopically imperceptible distinctions between immigrating bacteria and established Pst populations impact bacterial survival. By comparing and contrasting strategies used by Pst and Xhg, this study provides fundamental information about bacterial disease of leaves and reveals mechanisms used to reshape the host environment resulting in either a conducive or restrictive niche in the diseased host.

Results

Pst infection delays successful *S. Typhimurium* colonization of tomato leaves

Previously, we had shown that an established Xhg infection promotes the growth of newly arriving *S. Typhimurium* on tomato leaves (Dixon et al., 2022). To determine if another phytopathogen that causes water-soaking, Pst, also enhances *S. Typhimurium* persistence, we examined the impact of Pst infection on *S. Typhimurium* populations over time. As done previously, tomato leaves were infiltrated with phytopathogen, infection was allowed to proceed for 48 h post-infiltration (HPI), and *S. Typhimurium* was applied to the infected leaf surface as a droplet (Dixon et al., 2022). UV irradiation was used to distinguish surface localized *S. Typhimurium* from *S. Typhimurium* found within the apoplast (Dixon et al., 2022). Here, UV treatment was not a significant factor in bacterial populations ($p > 0.01$), and data from UV-treated and non-UV-treated samples were collapsed to create Figure 1. At the arrival site (Figure 1A), *S. Typhimurium* suspensions were absorbed equally amongst the three treatments, and no significant differences in *S. Typhimurium* populations were observed at 3 h post-arrival (HPA) between treatments or from the starting inoculum. Xhg infection resulted in 2–3 log higher apoplastic *S. Typhimurium* populations compared to the initial arriving population and 1–2 log higher populations compared to plants treated with Pst or water infiltration at 24, 48, and 72 HPA (Figure 1A). Contrastingly, *S. Typhimurium* populations did not significantly increase from starting inoculum levels in Pst-infected leaves until 48 HPA and remained lower than those in Xhg-infected leaves through 72 HPA (Figure 1A). Similar to,

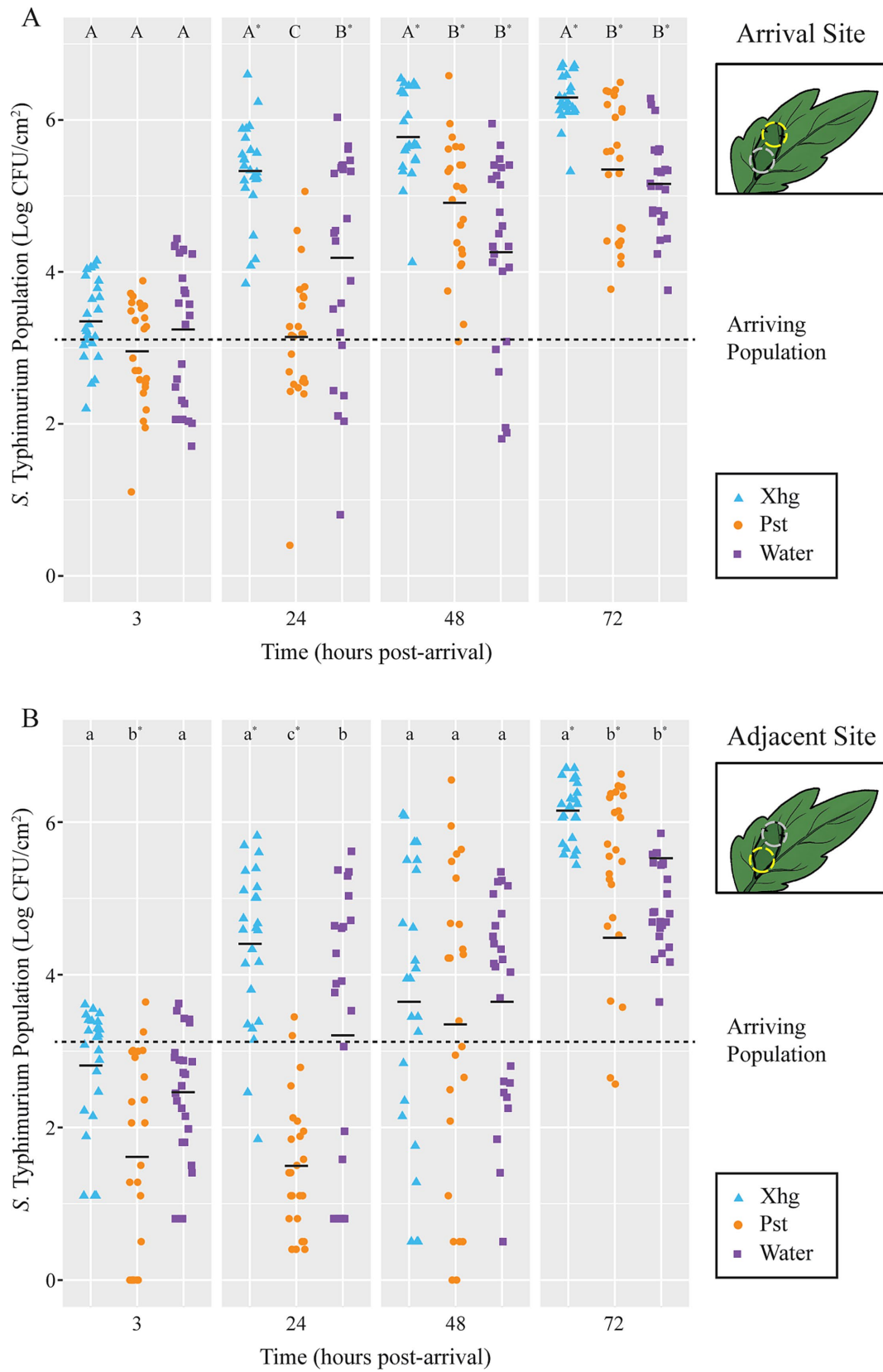


FIGURE 1

Immigrating *S. Typhimurium* have a delayed benefit from established Pst infection. *S. Typhimurium* populations were monitored 3, 24, 48, or 72 h after arrival on tomato leaves previously infiltrated with Xhg (48 HPI; cyan triangles), Pst (48 HPI; orange circles), or water (0 HPI; purple squares). Leaves were sampled at the *S. Typhimurium* arrival site (A) and a distinct adjacent site within the infiltrated area (B). Data from three independent experiments

(Continued)

FIGURE 1 (Continued)

are presented as log CFU/cm², and each symbol represents bacterial populations from one tomato leaf. Half of the leaves from each treatment and time point were treated with UV irradiation but data were collapsed as there was no significant difference between UV-treated and non-UV-treated samples ($p > 0.01$). The dashed line indicates the arriving *S. Typhimurium* population (3.1 log CFU/cm²). Means for each treatment at each time point are depicted with horizontal black lines. Letters denote significant differences between treatments within a single time point and leaf site, and asterisks indicate significant differences from the initial arriving population ($p < 0.05$). Combining three independent experiments, $n = 24$ leaves per treatment per time point.

but to a lesser extent than, Xhg infection, water congestion in healthy leaves also resulted in increased *S. Typhimurium* populations compared to the initial arriving population starting at 24 HPA (1–2 log; Figure 1A). However, as with Pst-infected leaves, water congested healthy leaves supported lower overall levels of *S. Typhimurium* compared to Xhg-infected leaves through 72 HPA (Figure 1A).

To examine migration of arriving bacteria, we monitored bacterial populations at an additional site within the infiltrated area, which we termed the adjacent site (Figure 1B). Bacterial populations at the adjacent site showed similar patterns as the arrival site with several notable differences. First, unlike at the arrival site, *S. Typhimurium* populations at the adjacent site in Pst-infected leaves are ~1.5 log smaller compared to the arriving population at 3 and 24 HPA (Figure 1B). Second, *S. Typhimurium* populations at the adjacent site on healthy water congested leaves did not grow from arriving population levels until 72 HPA (Figure 1B), instead of at 24 HPA as seen at the arrival site (Figure 1A). Third, although these experiments tend to show a relatively large amount of variation between samples and individual plants, all treatments displayed a wider range in *S. Typhimurium* population sizes at the adjacent site, when compared to the arrival site, at 48 HPA (Figures 1A,B). This 6-log range of bacterial population size at 48 HPA at the adjacent site resulted in no significant differences amongst treatments or compared to the arriving population at this timepoint. Phytopathogen populations were also monitored during these experiments and were not significantly different from one another at any time point at either the arrival site or the adjacent site ($p > 0.05$; Supplementary Figure S1).

Xhg- and Pst-infected leaves have similar macroscopic and microscopic symptoms

To identify differences in Xhg and Pst infection that could explain the delayed colonization of *S. Typhimurium*, we characterized multiple quantifiable phenotypes from Xhg- and Pst-infected leaves. To simulate a natural infection, tomato plants were dip-inoculated with Xhg and Pst suspensions and resulting disease symptoms were photographed at 1–4 days post-inoculation (DPI). To quantify disease symptoms, we developed the Leaf Lesion Detector application to quantify lesion numbers, size, and the percent infection observed over time in Xhg- and Pst-infected leaves (Figure 2). Representative images from 2 DPI leaves are shown at multiple stages of the application analysis to demonstrate functionality of this new software for potential use with other plant diseases. The details for image analysis are described in the methods below. The percentage of infected area is calculated as a ratio of lesion and leaf pixel counts. Conversion from pixel count to mm² is handled by multiplying a segment's pixel count by the ratio of known reference area to known reference pixel count. No significant differences in Xhg or Pst infection characteristics were

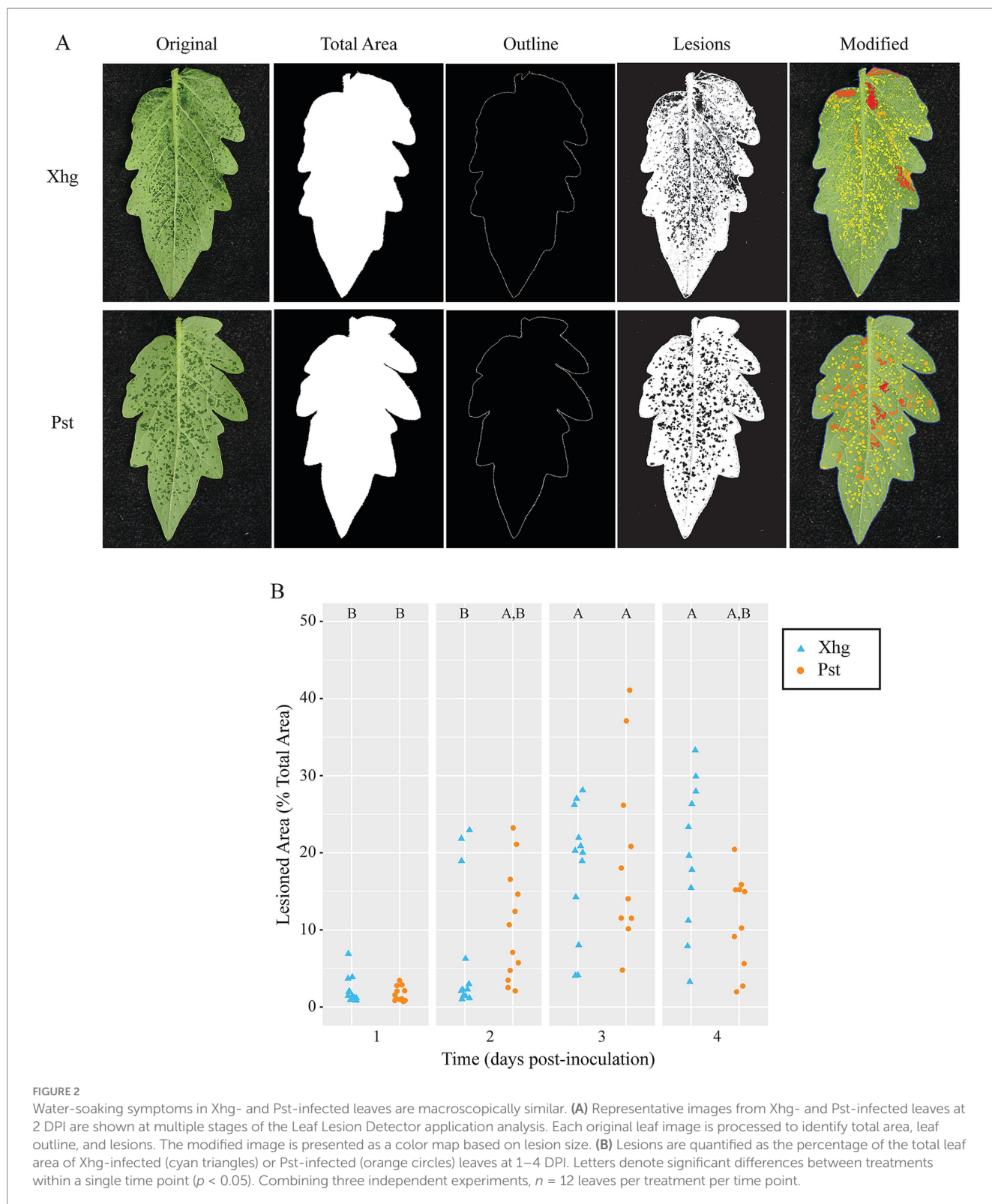
measured over the four-day time course using the Leaf Lesion Detector app (Figure 2B).

S. Typhimurium persistence in Figure 1 was quantified in infiltrated plants. To qualitatively examine plant disease under those conditions, infiltrated plants were imaged over time, and representative images from infection of each pathogen are shown in Figure 3A. No qualitative differences were observed when comparing infected leaves at each time point. Both Xhg- and Pst-infiltrated leaves showed patchy water soaking at 1DPI, complete water soaking of the infiltrated area by 2 DPI, a combination of water soaking and the beginnings of necrosis at 3 DPI, and drier, more necrotic tissue by 4 DPI (Figure 3A).

In addition to visible symptoms following infection, we measured both bacterial populations and cellular damage in infiltrated areas. As with symptomology, no differences were detected between Xhg- and Pst-infected leaves. Infiltrated pathogens reached a carrying capacity of 8.0–8.5 log CFU/cm² by 2 DPI, and bacterial populations were statistically equivalent at each time point examined (Figure 3B). Electrolyte leakage measured by conductivity was used as a proxy for cellular damage (Stall and Hall, 1984) throughout disease progression compared to leaves infiltrated with water. In parallel with lesion development, infection with both pathogens resulted in increasing levels of conductivity, and no differences were detected between Xhg- and Pst-infected leaves (Figure 3C).

Stomatal aperture patterns differ between Xhg- and Pst-infected leaves

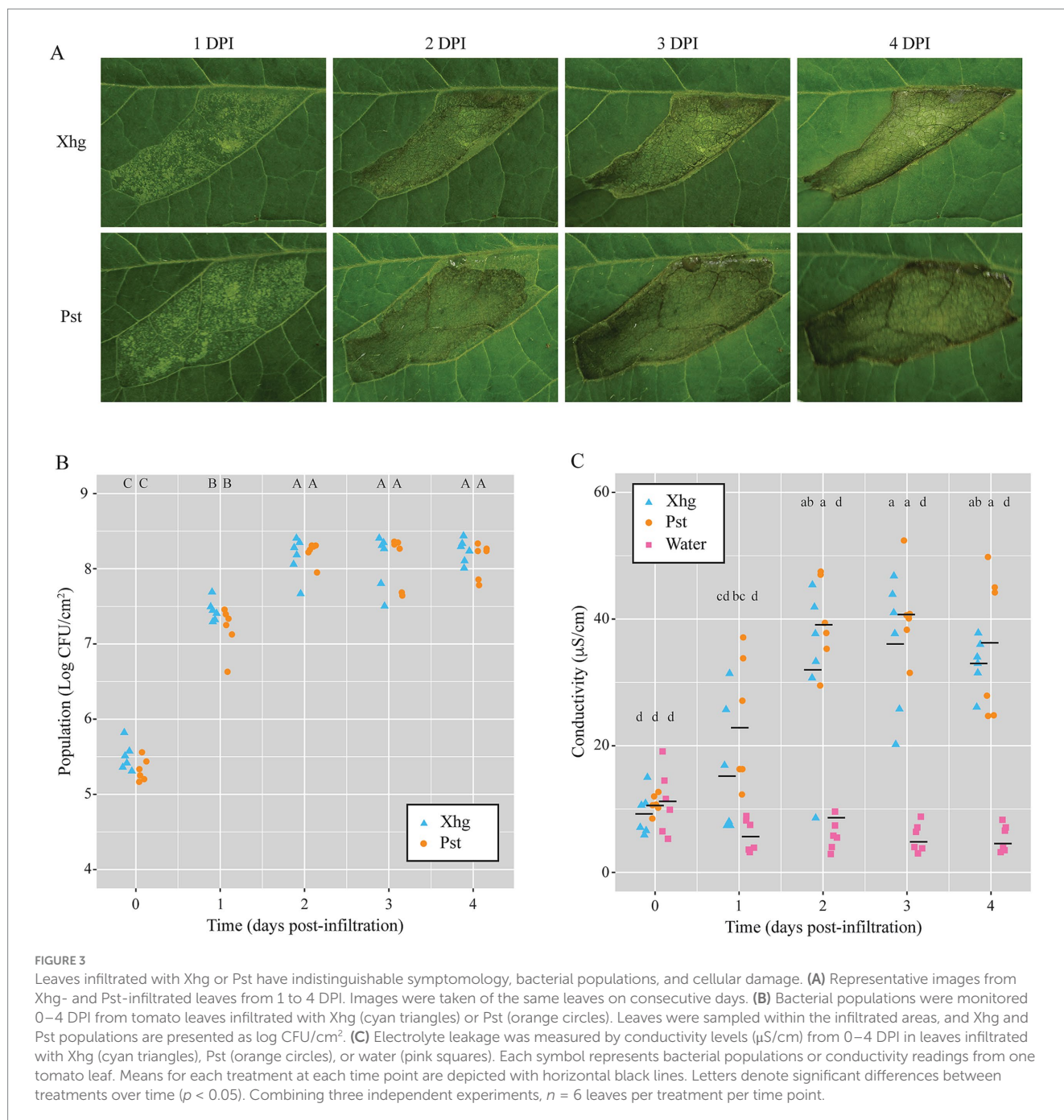
Previous work has shown that Pst opens and closes stomata of *Arabidopsis thaliana* or tomato leaves depending on the stage of infection (Roussin-Léveillé et al., 2022; Hu et al., 2022). To determine if stomatal aperture patterns could play a role in the different impacts of Xhg and Pst on *S. Typhimurium* success, we infiltrated leaves with phytopathogen or water and used a dental resin method to capture impressions of stomata over time. Stomatal apertures were measured using ImageJ and indicated by a ratio of width to length. The outline of stomata results in some measurement value for both length and width, making it impossible to get a ratio of 0.0. Thus, we considered a stomatal aperture ratio of 0.25 to be closed. Larger stomatal aperture ratios indicate more “open” stomata. Analysis of the resulting impression images demonstrated that while some temporal differences in stomatal apertures exist between Xhg- and Pst-infected leaves, infection with either pathogen results in open stomata at 48 HPI (Figure 4A), the point in time when *S. Typhimurium* cells were applied in our earlier experiments (Figure 1). All treatments had relatively closed stomata at 1 and 4 HPI (~ 0.25 aperture ratio; Figure 4A). Pst-infected leaves had open stomata by 24 HPI while Xhg-infected leaves had open stomata at 48 and 72 HPI (> 0.35 aperture ratio; Figure 4A). Water infiltration resulted in open stomata



at 24 and 48 HPI (> 0.35 aperture ratio), but stomata were closed at 72 HPI (~ 0.25 aperture ratio; [Figure 4A](#)).

In the *S. Typhimurium* survival experiments above ([Figure 1](#)), both *S. Typhimurium* and either phytopathogen were present on leaves at the same time while *S. Typhimurium* was not present in the stomatal aperture experiments in [Figure 4A](#). We hypothesized that

stomatal aperture regulation could be influenced by *S. Typhimurium*, and we repeated the stomata experiments with the addition of *S. Typhimurium* flagellin, a known signal for stomatal aperture movement ([Melotto et al., 2017](#)). As done above, leaves were infiltrated with a phyto-bacterial pathogen or water, and infection was allowed to proceed for 48 HPI. Then, flagellin was spotted on the surface of



infiltrated areas, similar to *S. Typhimurium* arrival in persistence experiments, and resin impressions were taken 1 or 4 h later (48 HPI + 1 and 48 HPI + 4). In persistence experiments (Figure 1), droplets of *S. Typhimurium* suspensions were absorbed into leaves by 3–4 h post-arrival, so these time points represent stomatal apertures at the time of *S. Typhimurium* arrival and absorption. As stated above, at 48 HPI, water-treated leaves had open stomata in the absence of flagellin (Figure 4A). However, in the presence of flagellin, water-treated leaves had closed stomata at both 48 HPI + 1 and 48 HPI + 4 (< 0.25 aperture ratios; Figure 4B). In contrast, both Xhg- and Pst-infected leaves had comparably open stomata in both the presence and absence of flagellin (> 0.35 aperture ratio; Figures 4A,B). Xhg-infected leaves had smaller stomatal apertures compared to

Pst-infected leaves at both time points post-flagellin treatment (Figure 4B).

Phytopathogens target potential competing bacteria in an *in vitro* growth inhibition assay

Our data demonstrates that Xhg infection creates a more conducive environment for *S. Typhimurium* persistence (Cowles et al., 2022; Dixon et al., 2022; Potnis et al., 2014, 2015) (Figure 1). To test the hypothesis that Pst could be directly inhibiting growth of other bacteria, we performed assays to study bacterial

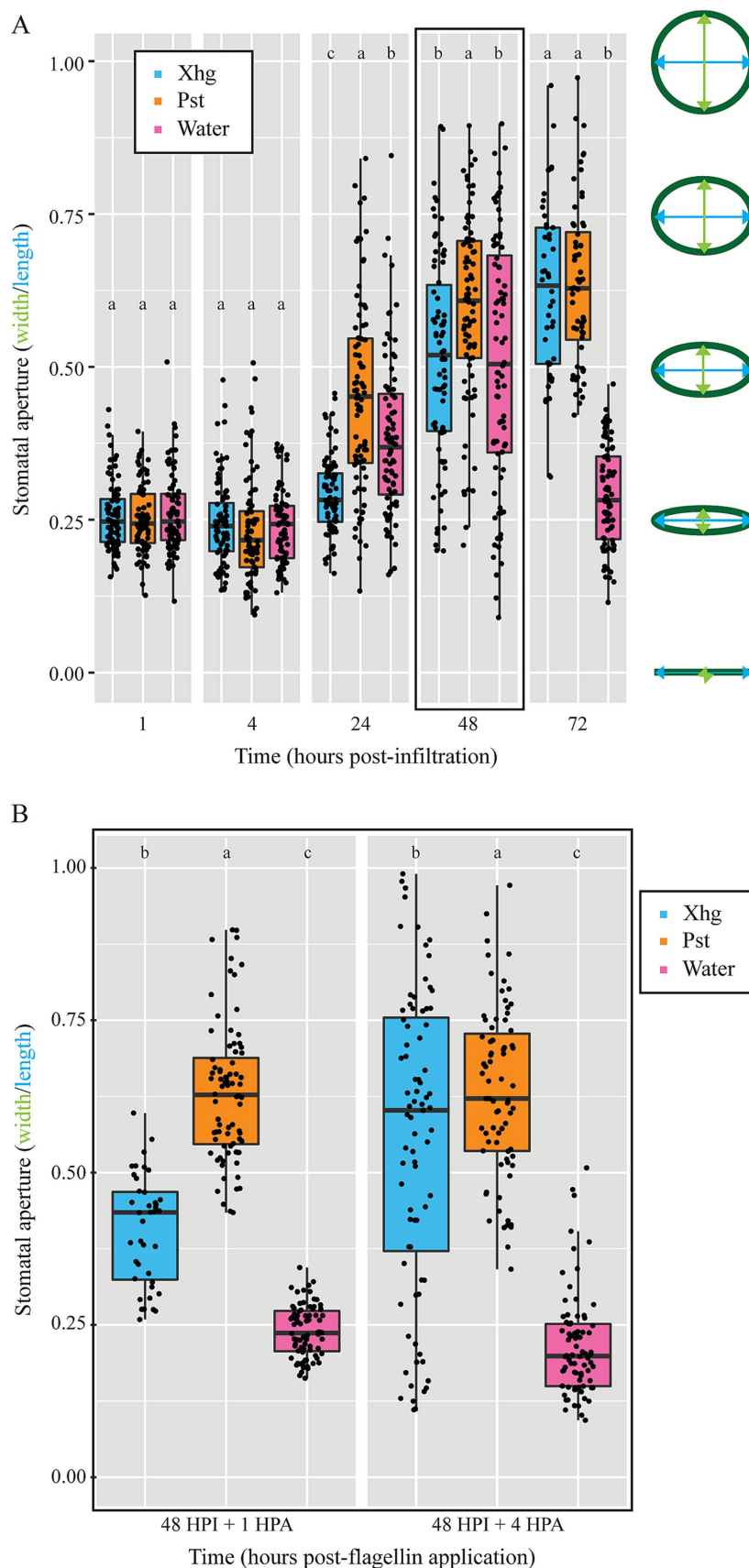


FIGURE 4
 Both Xhg- and Pst-infiltrated leaves have open stomata upon arrival of immigrating *S. Typhimurium* at 48 HPI. **(A)** Stomatal apertures were monitored at 1, 4, 24, 48, and 72 HPI in tomato leaves infiltrated with Xhg (cyan), Pst (orange), or water (pink). Apertures were measured using ImageJ and indicated by a ratio of width (green) to length (blue) as depicted on the right. The 48 HPI data are outlined in black to highlight the point when *S.*
 (Continued)

FIGURE 4 (Continued)

Typhimurium arrives at the infected area in other experiments. (B) Stomatal apertures were measured at 1 and 4 HPA of flagellin from leaves that had been previously infiltrated with Xhg (cyan), Pst (orange), or water (pink) 48 h earlier (48 HPI + 1 or + 4). Data from three independent replicates of each experiment are represented as boxplots with each symbol corresponding to one stomatal aperture ($n > 50$ per treatment per time point). Letters denote significant differences between treatments within a single time point ($p < 0.05$).

competition (Hood et al., 2010). In these experiments, *in planta* grown Xhg or Pst were mixed with target bacterial strains to assess growth inhibition. These assay conditions mimic the arrival of naïve bacteria to an established phytopathogen infection in leaves; bacterial strains are grown under the same conditions and mixed at the same ratios (1:1000; target strain to killer strain). Homogenized, healthy leaf tissue was used as a control for potential effects of plant factors. These data demonstrate that incubation with homogenized healthy leaf tissue had no impact on *S. Typhimurium* levels while Xhg- or Pst-infected tissue samples negatively affected *S. Typhimurium* populations (Figure 5A). Incubation with Xhg-infected tissue reduced *S. Typhimurium* populations by ~0.25 log while incubation with Pst-infected tissue resulted in ~1.25 log reduction in *S. Typhimurium* (Figure 5A).

To determine if *in planta* grown Pst affects other target bacteria, we performed additional competition assays with *in vitro* grown *S. Typhimurium*, Xhg, and Pst as the target strains. As seen above, Pst-infected tissue lowered *S. Typhimurium* populations by ~1.25 log while homogenized tissues from healthy plants had no effect (Figure 5B). As with the *S. Typhimurium* target, incubation of Pst-infected tissue with Xhg or Pst targets reduced populations by ~1 log (Figure 5B). While incubation with homogenized healthy leaf tissue had no impact on *S. Typhimurium* or Xhg populations, Pst target populations increased ~1 log when compared to incubation with water (Figure 5B).

A naïve, water-congested environment promotes phytopathogen success over pre-colonized tissues

With the knowledge that *in planta* grown Pst inhibits *S. Typhimurium*, Xhg, and Pst growth, we monitored the fate of newly arriving Xhg or Pst (immigrants) on leaf tissue with an established Xhg or Pst infection. As above for *S. Typhimurium*, leaves were infiltrated with Xhg or Pst, incubated for 48 HPI, and immigrant Xhg or Pst cells were applied as droplets to the infection site. One day after arrival on water-congested, healthy leaf tissue, both Xhg (Figures 6A,B) and Pst (Figures 6C,D) immigrant populations were 1–3 log larger compared to the initial arriving population, suggesting growth in healthy water-congested apoplasts that lacked established bacterial populations. UV irradiation to remove surface bacteria (Dixon et al., 2022) reduced both Xhg and Pst immigrant populations ~1.0 log compared to non-UV treated samples in water-congested leaves (Figure 6). However, UV-treated samples, at the arrival site, still had higher populations when compared to the initial arrival population, suggesting that the phyto-bacterial pathogen immigrants migrated to the UV-protected apoplast and grew (Figures 6A,C). UV-treated samples from the adjacent site were not significantly different from the arriving population (Figures 6B,D).

In contrast to increased immigrant populations on water-congested, healthy leaves, leaves with established Xhg or Pst infection, for the most part, either inhibited or reduced immigrant bacterial populations. In addition, unlike populations on water-congested, healthy leaves, UV irradiation had no impact on immigrant Xhg and Pst populations on infected leaf tissue (Figure 6), suggesting that the bulk of these bacteria had migrated into the UV-protected apoplast. Regardless of UV treatment, Xhg immigrants arriving on Xhg-infected leaves were not significantly different from the initial arriving populations (Figures 6A,B), indicating a lack of growth. Contrastingly, Pst immigrants arriving on Xhg-infected leaves were either the same as the arriving population or ~0.5 log higher (Figures 6C,D). While some Pst immigrants displayed growth from the initial arriving population, Pst populations were 1.5–2.5 log below levels seen in water congested, healthy tissue (Figures 6C,D), suggesting that Pst immigrants have some success on Xhg-infected leaves but replicate to greater numbers on naïve water congested tissue. Commonly, the Pst-infected environment had a more negative impact on immigrant bacteria, especially *S. Typhimurium* (Figure 1) and Xhg (Figures 6A,B), than the Xhg-infected leaf. For example, 1 day after arrival on Pst-infected leaves, Xhg immigrant populations at the adjacent site were reduced ~0.5–1.5 log compared to the initial arriving populations (Figure 6B). Comparably, 1 day after arrival on Pst-infected leaves, Pst immigrant populations at the adjacent site either remained at arriving population levels or were reduced by 1.0 log (Figure 6D).

Discussion

The leaf surface is a highly heterogeneous environment and can be characterized as a fragmented habitat driving the development of microbial communities (Doan et al., 2020; Fahrig, 2003; Schlechter et al., 2019). Factors that determine the maximum number of individuals on the leaf surface are host-driven (plant species, water pooling, or nutrient leaching through the cuticle) or bacteria-driven (environmental stress response, motility, or aggregate formation). An immigrant's fate on the leaf surface is determined by the luck of arriving at or near an oasis (Remus-Emsermann and Leveau, 2010) or with others (Monier and Lindow, 2003; Remus-Emsermann et al., 2012). One avenue used by phytopathogenic bacteria to infect leaves is entry to the leaf interior through stomata, the gas exchange portal. Early in infection, both Xhg and Pst transform the air-filled apoplast to an aqueous environment (reviewed in Xin et al., 2016). Based on our results, bacteria that arrive on a leaf as immigrants and attempt to establish themselves in the apoplast appear to encounter fundamentally different niches upon arrival to a naïve host compared with a plant hosting a previously established infecting population. Furthermore, our data show that the identity of the established population also influences the fitness outcomes for the immigrating bacteria.

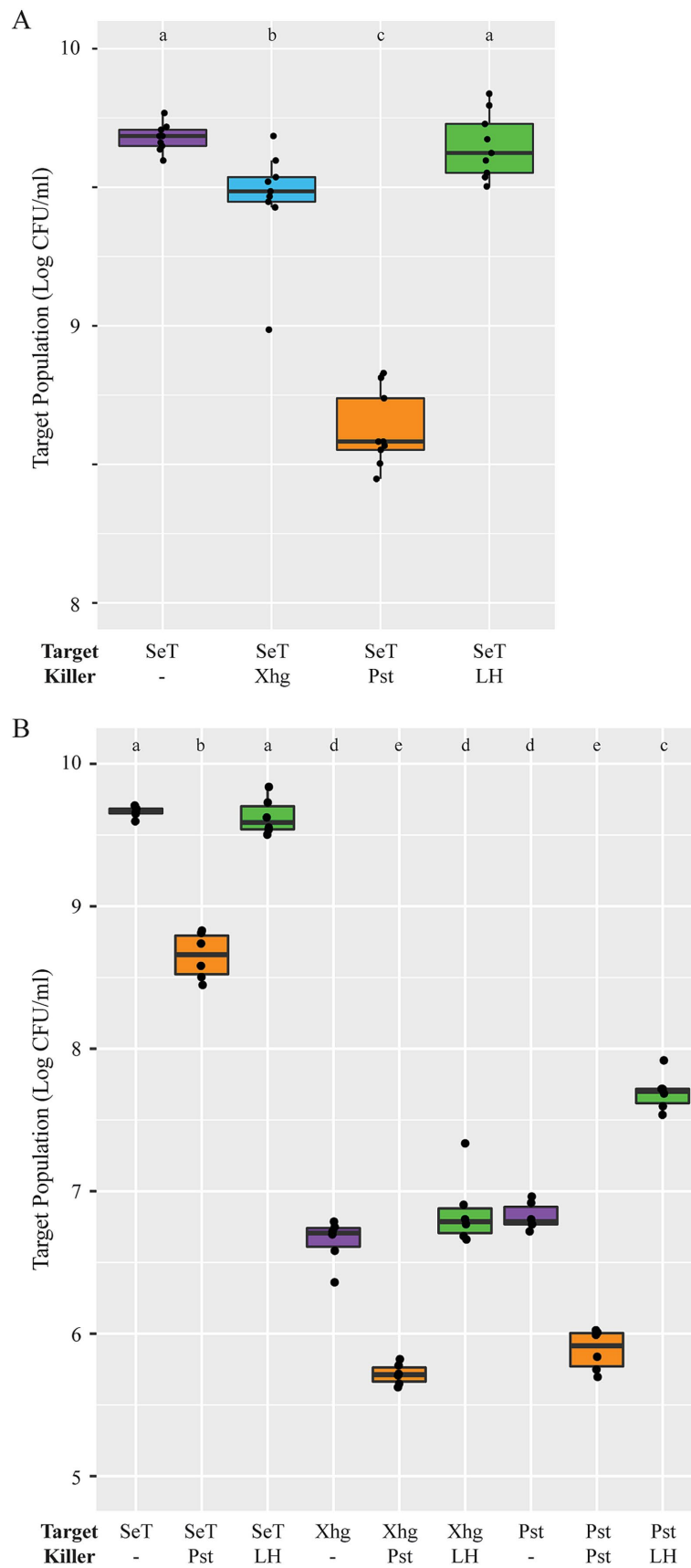


FIGURE 5
In planta grown Pst inhibits *in vitro* grown *S. Typhimurium*. **(A)** Using a bacterial competition assay, *S. Typhimurium* populations were measured after 24-h incubation with water (purple), *in planta* grown Xhg (cyan), *in planta* grown Pst (orange), or healthy leaf homogenate (green). **(B)** Assays were repeated with three target bacterial strains (*S. Typhimurium*, Xhg, and Pst) and three treatment conditions (water, purple; *in planta* grown Pst, orange; healthy leaf homogenate, green). Target bacterial population data from two independent experiments are presented as log CFU/mL in boxplots ($n = 6$). Letters denote significant differences between treatments ($p < 0.05$).

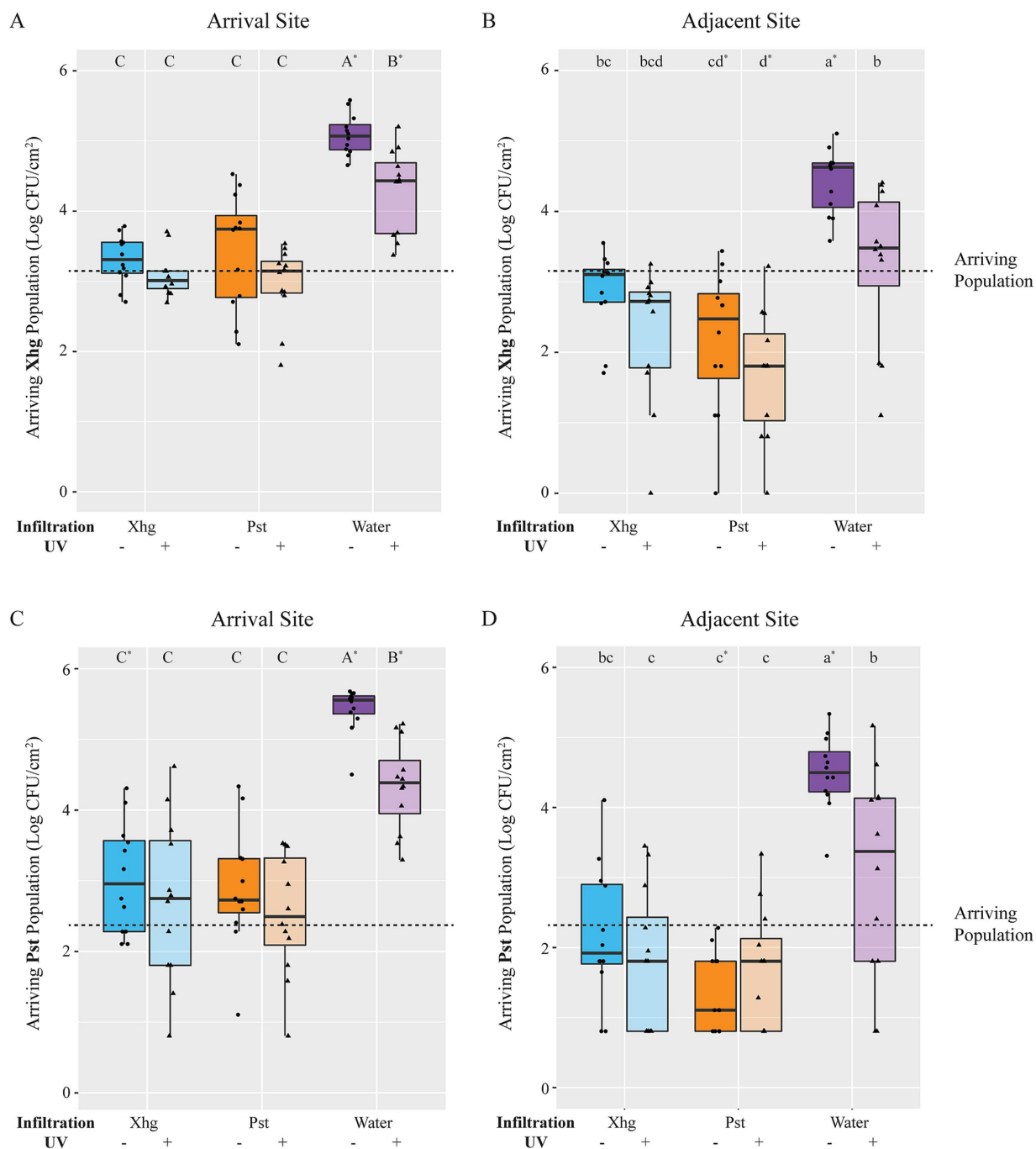


FIGURE 6
 The fate of immigrating bacteria depends on the identity of the established infection. Xhg (A,B) and Pst (C,D) populations were monitored 24 h after arrival on tomato leaves previously infiltrated with Xhg (48 HPI; cyan), Pst (48 HPI; orange), or water (0 HPI; purple). Leaves were sampled at the arrival site (A,C) and a distinct adjacent site within the infiltrated area (B,D). Data from three independent experiments are presented as log CFU/cm² in boxplots, and each symbol represents bacterial populations from one tomato leaf (*n* = 12 leaves per treatment per time point). Half of the leaves from each treatment and time point were treated with UV irradiation and distinguished here with color shading. The dashed line indicates the arriving bacterial population (3.1 log CFU/cm²). Letters denote significant differences between treatments within a single leaf site for each bacterium separately, and asterisks indicate significant differences from the initial arriving population (*p* < 0.05).

Nutrient availability in the apoplast

Upon arrival to a healthy, water-congested apoplast, all three examined bacteria, whether phytopathogenic or not, demonstrated a two-log increase in growth from the initial inoculum population

(Figures 1, 6). The similar fate for bacteria on a healthy, yet water-congested, host suggests that uptake of the droplet containing bacteria concurrently allows bacterial entry to the apoplast. In addition, bacteria that reach the apoplast have access to some degree of available nutrients, even *S. Typhimurium* which does not manipulate the host

niche. A “dry” healthy apoplast is mainly air-filled with a thin water film over cell surfaces. Apoplastic nutrients are thought to be in a bound state, attached to cell surfaces, or within surrounding cells, and relatively unavailable to invading bacteria (Roussin-Leveillee et al., 2024; Melotto et al., 2008). It is hypothesized that an influx of water in the “wet” healthy apoplast may disrupt metabolite uptake and result in a dysregulation of metabolite partitioning with higher than normal water-soluble metabolite concentrations in the apoplast (Roussin-Leveillee et al., 2024; Gentzel et al., 2022). This access to nutrients could lead to the observed increases in *S. Typhimurium*, Xhg, and Pst growth (Figures 1, 6). The temporary relief from nutrient restriction appears to be nondiscriminatory and available to any bacterium lucky enough to arrive in a water droplet on the water-congested leaf.

Unlike the transient nature of abiotic water congestion described above, pathogen-induced water soaking is maintained over days and represents a more complex system of pathogen manipulation of the host and the host response. As with abiotically water-congested leaves, *S. Typhimurium* replicates within the protected niche of the Xhg-infected apoplast within the first 24 h of arrival on infected tissue (Figure 1). Contrastingly, *S. Typhimurium* does not demonstrate growth in Pst-infected tissue until 48 HPI and does not reach the same level as *S. Typhimurium* populations in Xhg-infected tissue at any examined time point (Figure 1). There are also differences in the fates of immigrant phytopathogens on infected tissue, compared with abiotically water-congested leaves. Neither Xhg nor Pst immigrants increase from arriving population levels on Xhg- or Pst-infected leaves (Figure 6). The static nature of these populations could represent lack of replication, slow replication (that is not detectable within 24 HPI), or an equal rate of replication to death, resulting in no net increase in population levels. We hypothesize that the differential impact of established phytopathogens and/or infections on immigrant success results from differences in available resources within the apoplast. In support of the idea that competition plays an important role in this niche, we showed that *in planta* grown Pst inhibits growth of multiple bacteria, including *S. Typhimurium*, Xhg, and even Pst itself (Figure 5). Monopolization of resources within the infection court by established bacteria could lead to direct competition for space and/or nutrients.

The formation of distinct niches based on the identity of the infecting phytopathogen may be the result of the available nutrient profile. As mentioned above, water congestion itself leads to a misregulation of metabolite partitioning (Roussin-Leveillee et al., 2024; Gentzel et al., 2022) and growth of *S. Typhimurium* (Figure 1). Water soaking due to infection can also influence plant metabolism directly to the benefit of the resident organism. Phytobacterial pathogens such as Pst and *Ralstonia solanacearum* use secreted effectors to manipulate their host to create a more nutritionally favorable environment or increase specific nutrient availability (Ward et al., 2010; Xian et al., 2020). Multiple additional phytopathogens also hijack plant metabolism to shift source leaves into sink leaves, providing the pathogens with access to nutrients (McIntyre et al., 2021; Rodenburg et al., 2019; Doehlemann et al., 2008; Gohlke and Deeken, 2014). Alternatively, established Xhg populations may have distinct nutritional requirements from *S. Typhimurium*, allowing both bacteria to thrive, while established Pst populations have overlapping nutritional needs, resulting in competition for resources. Future experiments examining the metabolite profiles of the infected apoplasts could reveal details of this mechanism.

Stomatal response and bacterial entry

Without cell wall degrading enzymes, bacteria like *S. Typhimurium* have restricted access to the leaf interior through natural openings such as stomata, hydathodes, and wounds (Golberg et al., 2011; Chahar et al., 2021). Although the primary function of stomata is the regulation of gas exchange and water retention, stomatal cells (guard cells) can recognize conserved microbe associated molecular patterns (MAMPs) and close the opening to reduce or prevent bacterial entry (Melotto et al., 2006; Melotto et al., 2017; Melotto et al., 2008; Daszkowska-Golec and Szarejko, 2013). We see this closure response in our experiments when *S. Typhimurium* flagellin is added to the surface of tissue infiltrated with Xhg or water (Figure 4). Some bacterial phytopathogens that infect the apoplast have evolved toxins that open stomata, increasing access to the leaf interior (reviewed in Melotto et al., 2017; Melotto et al., 2008). Published works describe a model where Pst uses stomatal apertures as an entryway; using T3SS effectors to open stomata for bacterial entry and close the door behind them to create a water-soaked environment and reduce evaporation (Melotto et al., 2006; Roussin-Léveillé et al., 2022; Hu et al., 2022). We hypothesized that the closed stomata in Pst-infected tissue may prevent *S. Typhimurium* entry when it arrives at 48 HPI, thus delaying *S. Typhimurium* success in this environment. However, unlike published works in *A. thaliana* (Roussin-Léveillé et al., 2022; Hu et al., 2022), our data demonstrate that from 24 HPI to 72 HPI, Pst-infected tomato leaves maintain open stomata (Figure 4). We predict that differences between our results here and published results (Roussin-Léveillé et al., 2022; Hu et al., 2022) are due to multiple differences in the investigated plant—microbe interactions. We anticipate that the primary driver of these disparities come from differences in the Pst strains used in the respective experiments. Pst DC3000 is pathogenic towards some tomato cultivars and *A. thaliana* while the Pst NY15125 strain used here is nonpathogenic towards *A. thaliana* (Kraus et al., 2017). There are also known differences between these two bacterial strains in both T3SS effector profiles as well as virulence towards tomatoes, depending on the tomato host (Kraus et al., 2017; Mazo-Molina et al., 2019). As T3SS effectors are vital for manipulating stomatal immunity, it is not surprising that profile differences could result in differential effects on stomata. While these results point to subtle differences between the two phytopathogens in terms of plant response to environmental cues, *S. Typhimurium* has access to open stomata in both Xhg- and Pst-infected leaves. Thus, differential regulation of stomata does not explain why Pst fails to support *S. Typhimurium* colonization as quickly as Xhg.

Dispersal within host tissue

For more than a century, plant pathologists have used disease severity indices to rate gross aspects of infection that are generally based on the percent area with visible symptoms (for review Bock et al., 2022). Yet, this disease quantification is a crude characterization of changes to the infected host and reveals nothing of the infected population's current activities and dispersal since the bacterial pathogen is rarely isolated from diseased tissue. To quantify changes to the host following infection, we created a new software application, Leaf Lesion Detector (LLD). This application is publicly available and

provides a new tool for researchers examining plant disease. Here, LLD was used to quantify disease progression in Xhg- and Pst-infected leaves (Figure 2) and demonstrated that both phytopathogens produced quantitatively and qualitatively similar lesions, in abundance and size, over the course of infection. While no differences were noted that would explain the differential success of *S. Typhimurium* in either dip-inoculated or infiltrated plants, heterogeneous patches of water soaking developed in both Xhg- and Pst-infiltrated leaves at 1 DPI (Figure 3A). The process of infiltration immediately produces a homogeneously water-congested area that quickly dissipates within several hours. The resulting heterogeneity of apoplast water soaking just 1 day later suggests that the phytopathogens may form microcolonies or that infection of host cells is not in synchronicity before water-soaking floods the entire infected area by 2 DPI (Figure 3A). The formation of distinct subpopulations occurs in *P. syringae* pv. *phaseolicola* in the apoplast of bean leaves where bacteria are found clustered in microcolonies after infiltration (Rufian et al., 2018). Multispecies interactions within these subpopulations even support the success and dispersal of non-pathogenic strains (Rufian et al., 2018). Thus, although symptomology of Xhg- and Pst-infected leaves appears macroscopically similar, the infected and colonized apoplast reflects a more complex environment that requires further exploration to identify phytopathogen-specific mechanisms of niche establishment and host manipulation.

In terms of space, the carrying capacity of bacteria that colonize leaf surfaces have been well documented, at least for the phytopathogen Pst and the non-pathogenic *Pantoea agglomerans* (Remus-Emsermann et al., 2012; Woody et al., 2007; Wilson and Lindow, 1994a,b, 1995; Nix et al., 2009; Knief et al., 2010; Kinkel et al., 2000). Despite this wealth of information, the carrying capacity within the apoplast remains poorly understood. We predict that the carrying capacity of the apoplast is dynamic and changes as the state of the host fundamentally transforms following infection. Our results indicate that tomato leaves have similar carrying capacities for Pst and Xhg as both phytopathogens reach plateaus at approximately the same level and time point in infection (8.0–8.5 log CFU/cm²; Figure 3). Despite this similarity, Xhg-infection enhances persistence of immigrating bacteria, such as *S. Typhimurium*, while Pst-infection does not (Figures 1, 6). While these results indicate that space restriction does not appear to be a primary mechanism for impacting immigrant success, it again suggests that infection or established status with the different genera results in unique niches within the same host.

Water congestion may also impact bacterial migration and dispersal within host tissues. Bacteria utilize swimming and other forms of motility to reach preferential niches, responding to environmental cues to reach essential nutrients (Dixon et al., 2022; Haeefe and Lindow, 1987; Lindow et al., 1993; Leveau and Lindow, 2001; Berger et al., 2009). Here, we show that, unlike *S. Typhimurium* (Figure 1), both Xhg and Pst remain susceptible to UV (Figure 6), indicating that the phytopathogens spend more time on the leaf surface than *S. Typhimurium*, even once water soaking has begun. Bacterial phytopathogens use motility as a mode of dispersal within and between plants (Monier and Lindow, 2003; Haeefe and Lindow, 1987; Remus-Emsermann et al., 2012; Kinkel, 1997), and Xhg and Pst may be transitioning in and out of the apoplast via stomata or through damaged tissue once lesions have developed. Thus, the observed UV susceptibility could reflect increased attempts of the phytopathogens to migrate to distal sites within or on the infected host. In contrast, our

data suggest that, once within the apoplast, few *S. Typhimurium* cells, if any, migrate back to the leaf surface. We also found that Pst infection appears to inhibit migration to the adjacent site for all arriving bacteria (*S. Typhimurium*, Xhg, or Pst; Figures 1, 6). Previous results have suggested that Pst infection transforms the apoplast, either building physical barriers through biofilm production or manipulating the host response to prevent migration once inside the leaf tissue. For example, Pst infection in *A. thaliana* leads to restricted vascular flow to the infection site, which could also limit bacterial migration (Freeman and Beattie, 2009). Similarly, the ROS response to phyto-bacterial infection may link bacterial cells to cell wall components within the apoplast (Soylu et al., 2005), inhibiting bacterial movement. A phytopathogen-specific mechanism during infection would explain why movement of immigrating bacteria is restricted in Pst-infected tissue while Xhg-infected tissue allows bacteria to move more freely.

To summarize, the leaf surface and apoplast present a complex and dynamic environment for bacterial communities, influenced by both host and bacterial factors. Previous studies have demonstrated that the fate of immigrant bacteria is shaped by arrival site conditions (Monier and Lindow, 2003, 2004; Barak et al., 2011). Here, we have added that the presence of established bacterial populations can create distinct niches and competition for resources among bacterial community members. We demonstrate that abiotic water congestion, pathogen-induced water soaking, and interbacterial competition play crucial roles in bacterial colonization and survival. Further research is needed to dissect the molecular mechanisms underlying these processes and develop targeted strategies for disease control. A more comprehensive understanding of the bacterial infection and colonization mechanisms in plant tissues could ultimately inform crop protection strategies, enhance agricultural sustainability, and improve food safety.

Materials and methods

Bacterial strains, media, and culture conditions

Strains used in this study are shown in Table 1. Kanamycin resistant Xhg was created by transforming Xhg 444 wildtype strain with pKTKan (Miller et al., 2000). Bacterial cultures were grown in lysogeny broth (LB) for *S. Typhimurium*, nutrient broth (NB) for Xhg, and nutrient yeast extract dextrose broth (NYD) for Pst. All bacterial strains were incubated at 28°C with shaking at 200 rpm. The antibiotics nalidixic acid (Nal), kanamycin (Kan), and gentamicin (Gent) were used at concentrations of 20, 50, and 10 µg mL⁻¹, respectively.

Plant inoculation

Solanum lycopersicum (tomato cultivar MoneyMaker) seeds were purchased commercially (Eden Brothers). This study complies with the relevant institutional, national, and international guidelines and legislation for experimental research on plants. Seedlings were cultivated in Professional Growing Mix (Jolly Gardener Pro Line, Carlin Sales) with a 16 h photoperiod at 24°C for 5 weeks. For colonization assays, Xhg and Pst bacterial

TABLE 1 List of strains.

Strain designation	Genotype	References or sources
JDB1022	<i>S. enterica</i> serovar Typhimurium 14,028 s; Kan ^R at the <i>attTn7</i> site	Cowles et al. (2022)
JDB1470	<i>X. hortorum</i> pv. <i>gardneri</i> 444; Nal ^R	Cowles et al. (2022)
JDB1504	<i>X. hortorum</i> pv. <i>gardneri</i> 444 + pKTKan; Kan ^R	This study
JDB1514	<i>P. syringae</i> pv. <i>tomato</i> NY15125; Kan ^R	Martin lab
JDB1515	<i>P. syringae</i> pv. <i>tomato</i> NY15125; Gent ^R	Martin lab

cultures were grown for 2 days in NB or NYD, respectively, at 28°C, and *S. Typhimurium* cultures were grown overnight in LB at 28°C. Bacterial strains were normalized to an optical density at 600 nm (OD₆₀₀) of 0.2 (for *S. Typhimurium* and Pst strains) and 0.3 (for Xhg) in sterile water. These OD₆₀₀ values correspond to a bacterial population level of ~10⁸ CFU/mL for the respective strains. For dip inoculation, normalized Xhg and Pst cultures were diluted 1:200 in sterile water for an inoculum level of ~5 × 10⁵ CFU/mL. Prior to dip inoculation, 0.025% Sil-Wett was added to the bacterial inoculum. Tomato plants were dip-inoculated by inverting plants in the bacterial inoculum for 30 s with gentle agitation to prevent bacterial cell settlement. Plants were incubated at high humidity for 48 h in lidded, plastic bins under grow lights with a 12 h photoperiod at room temperature (~26°C). After 48 h, plants were exposed to low humidity conditions (bin lids were removed) during the day and high humidity conditions (bin lids were replaced) during the night. For infiltration experiments, two leaflets on the third true leaf of MoneyMaker tomato plants were infiltrated with Xhg or Pst at ~1 × 10⁷ CFU/mL, prepared as above for dip inoculation experiments, following published protocols (Cowles et al., 2018, 2022). Bacterial solutions were infiltrated into the abaxial leaf surface using a plastic, disposable 3 mL, needleless syringe (Fisher Scientific), and, for some experiments, infiltrated zones were delineated with permanent marker. Infiltrated plants were incubated in lidded, plastic bins as described above. For disease comparison of infiltrated plants, non-destructive images of leaflets were taken at multiple days post-infiltration using a Canon PowerShot ELPH 1901S camera.

Image collection and processing

At multiple days post-dip inoculation, individual leaflets were removed, submerged in water for 10 s (to increase lesion visibility), gently patted dry with kimwipes, and imaged for lesion quantification on a black velvet background using a Canon PowerShot ELPH 1901S camera. Images were cropped to center the leaflet and remove background. Leaf area and lesion analysis was performed with the custom image processing software: Leaf Lesion Detector v2023.2.0 (LLD), developed for this project. LLD automates manual image segmentation procedures (Pride et al., 2020). The Leaf Lesion Detector

application segments images using a series of hue, saturation, value (HSV) thresholding operations, and contour finding (van der Walt et al., 2014) on greyscale-converted images, both of which use empirically predetermined, but configurable pixel-value limits. Each leaf and reference image are processed as follows: (1) Segment reference area by thresholding, applying noise reduction, then counting resulting pixels (not shown). (2) Segment leaf area by thresholding and contour finding (Figure 2A, Total Area and Outline). (3) Segment lesion area by thresholding, contour finding, labelling all lesions and summing the area for all lesions above the configured minimum lesion size threshold pixel count (Figure 2A, Lesions). All the segmentations are combined and a color map applied to the lesions by size to create the final image (Figure 2A, Modified). If the total lesion area of a leaf exceeds 3.5%, the image is reprocessed with a more stringent lower bound (supplied in the configuration) for lesion size. After testing several different cutoff values on a range of test images, 3.5% was chosen as it appeared to give the best trade-off between maximizing detection and minimizing false positives. Results from LLD visually correspond to leaf lesions and correlate with manually produced results (R² = 0.95). The application is publicly available at this url: <https://leaf-lesion-detector.streamlit.app/>. The code and the configuration settings used in this work are also publicly available on GitHub (pending publication): <https://github.com/UW-Madison-DSI/plant-pathology-image-processor>.

Immigrant arrival

S. Typhimurium, Xhg, and Pst cultures were grown as described above, normalized to OD₆₀₀ = 0.1, and diluted in sterile water for a final concentration of ~10⁶ CFU/mL. Normalized and diluted immigrant cultures were applied as 15 µL droplets to the adaxial surface of infiltrated leaf tissue, which included leaflets infected with Xhg or Pst for 2 DPI, as well as leaflets freshly infiltrated with sterile water, as done previously (Dixon et al., 2022). The droplet “arrival site” was denoted with permanent marker and is depicted in Figure 1 for clarity. Inoculated plants were incubated at room temperature for 3 h to allow for droplet absorption and then moved under grow lights until sampling. Bacterial inoculums were diluted and plated for population counts.

Bacterial population sampling

Bacterial populations on leaves were determined as described (Cowles et al., 2018, 2022; Dixon et al., 2022). Briefly, at indicated times, two individual leaflets were removed from each plant, and the adaxial surface of one leaflet per plant was treated with 254 nm UV radiation (Stratalinker UV Crosslinker 1800) at 150,000 µJ/cm² (for *S. Typhimurium*) or 300,000 µJ/cm² (for Xhg or Pst). Irradiated leaflets were chosen at random for each plant. Two 0.79 cm² leaf discs were taken from each leaflet using a surface sterilized cork borer. One disc was removed from site of droplet application and designated as the arrival site (Figure 1). The other disc was sampled at an adjacent, nonoverlapping region within the infiltration zone and termed the adjacent site (Figure 1). Samples from four plants per treatment per time point were individually homogenized in 500 µL of sterile water in microfuge tubes

using a 4.8 V rotary tool (Dremel, Mt. Prospect, IL) with microcentrifuge tube sample pestle attachment (Fisher Scientific). Homogenates were diluted and plated to enumerate bacteria on LB Kan (for *S. Typhimurium*), NB Nal or NB Kan (for Xhg), or NYD Kan or Gent (for Pst) agar plates. Resulting colonies were counted after overnight incubation at 37°C (for *S. Typhimurium*) or after incubation for 2–3 days at 28°C (for Xhg and Pst) to determine bacterial populations. Remaining leaf homogenate was incubated with media amended with kanamycin to enrich for immigrating bacteria below the limit of detection in the above plating method (Dixon et al., 2022). Enrichments were plated on media with kanamycin after 1 day (*S. Typhimurium*) or 2–3 day (Xhg and Pst) incubation at 28°C. Lack of growth was recorded as a zero for population graphs while growth was indicated by data points halfway between the original limit of detection (0.7 log CFU/cm²) and zero. Experiments were performed with three biological replicates.

Electrolyte leakage

Plants were infiltrated with Xhg, Pst, or water alone, as described above. Leaf tissue samples were collected at 0, 1, 2, 3, and 4 DPI for bacterial populations and electrolyte leakage measurements. Four leaf discs were taken from the infiltrated zones of leaflets from the third true leaf of each plant. One disc was used to enumerate bacterial populations (as described above), and three discs were pooled and quantified for changes in electrolyte leakage (conductance) as previously described (Harrod et al., 2022; Kessens et al., 2018). Briefly, leaf discs were placed in a 12-well plate containing 4 mL sterile water per well, three leaf discs per well. Leaf discs were washed for 30 min with gentle agitation, and the water was removed and replaced with 4 mL fresh, sterile water. Baseline conductance values from each well were immediately measured using an ECTestr11 + MultiRange electrical conductance probe. Plates were incubated under grow lights for 6 h, and final conductance values were collected from each well. Data are expressed as differences between baseline and final conductance readings as a proxy for cellular damage and electrolyte leakage. Experiments were performed with three biological replicates.

Stomatal aperture imaging and analysis

Plants were infiltrated with Xhg, Pst, or water alone, and stomatal apertures were measured using a dental resin technique (Geisler et al., 2000; Nir et al., 2017). Bacterial suspensions were prepared as described above and infiltrated as ~1 cm² areas on leaflets from the third true leaf. To capture stomatal apertures at 1, 4, 24, 48, and 72 HPI, impressions of the leaf surface were taken using light-body vinylpolysiloxane (VPS) dental resin. Resin was applied in a thin layer to the adaxial surface of leaves over the infiltrated area, dried for ~5 min, and then removed. Resin impressions were coated with clear nail polish. Once dried and removed, the nail polish mirrors the leaf surface impression. Nail polish imprints were placed on cover slips, and stomata were imaged with a Cytation 7 Cell Imaging Multi-Mode Reader (Biotek). Infiltrated areas on leaflets were outlined with permanent marker, which transfers to both the resin and nail polish and allows for identification of infiltrated tissue under the microscope. Stomatal apertures were measured within infiltrated areas using ImageJ (Schneider et al., 2012) ($n > 100$ stomata per

treatment), and resulting length to width ratios are presented in Figure 4. To examine stomatal responses to flagellin, leaflets were infiltrated with Xhg, Pst, or water, as described above. At 48 HPI, purified *S. Typhimurium* flagellin (50 ng/mL; Fisher Scientific) was applied as a droplet to the adaxial surface of the infiltrated areas. Resin impressions were taken at 1 or 4 HPA, and stomatal apertures were measured as described above. Experiments were performed with three biological replicates.

Bacterial growth inhibition assays

Plants were infiltrated with Xhg, Pst, or water alone, as described above. At 48 HPI, four 0.79 cm² leaf discs were taken from infiltrated areas using a surface sterilized cork borer, pooled, and homogenized in 500 µL of sterile water. This procedure was repeated for each treatment to collect concentrated homogenates to act as the “killer” suspensions. Target strains were prepared as described above for plant inoculations except that strains were normalized to OD₆₀₀ = 0.5. Normalized target strains were mixed with concentrated killer strain homogenates at a ratio of 1:1000. Killer-target mixtures, as well as killer and target strains alone, were spotted to agar plates (LB for *S. Typhimurium*, NB for Xhg, or NYD for Pst) and incubated at 28°C for 24 h. Agar cores were then excised from plates and vortexed thoroughly in 1 mL sterile water to collect bacterial cells. Suspensions were diluted and plated for bacterial enumeration. Resulting colonies were counted after overnight incubation at 37°C (for *S. Typhimurium*) or after incubation for 2–3 days at 28°C (for Xhg and Pst) to determine bacterial populations. Experiments were repeated as two biological replicates with three technical replicates each.

Statistical analysis

All statistical analyses were performed using R software (version 2.14.1; R Development Core Team, R Foundation for Statistical Computing, Vienna, Austria¹) as described (Kwan et al., 2015). Three biological replicates were performed for each experiment. The ANOVA and Tukey's HSD test were used to compare treatments within each time point for most experiments and over time for carrying capacity and conductivity experiments in Figure 3. Normality and homogeneity of variance for all data were confirmed by graphing residuals using Q-Q and density plots. The one sample *t*-test was used to compare bacterial populations to the initial arriving populations on tomato leaves. Results were considered statistically significant at $p < 0.05$.

Data availability statement

The raw data supporting the conclusions of this article will be made available by the authors, without undue reservation.

¹ <http://www.R-project.org>

Author contributions

KC: Data curation, Formal analysis, Investigation, Methodology, Supervision, Visualization, Writing – original draft, Writing – review & editing. AI: Formal analysis, Investigation, Software, Writing – review & editing. IM: Formal analysis, Software, Supervision, Writing – review & editing. EG: Investigation, Writing – review & editing. DN: Investigation, Writing – review & editing. SZ: Investigation, Writing – review & editing. JB: Conceptualization, Funding acquisition, Resources, Supervision, Writing – review & editing.

Funding

The author(s) declare that financial support was received for the research, authorship, and/or publication of this article. This work was funded by the Food Research Institute, UW-Madison and USDA—Hatch grant.

Acknowledgments

We would also like to thank G. Martin (Cornell Univ.) for marked Pst NY25 strains and acknowledge JDB's lab members for helpful discussions.

References

- Agrios, G. (Ed.) (2005). *Plant pathology*. Burlington, MA: Elsevier Academic Press.
- Barak, J. D., Kramer, L. C., and Hao, L. Y. (2011). Colonization of tomato plants by *Salmonella enterica* is cultivar dependent, and type 1 trichomes are preferred colonization sites. *Appl. Environ. Microbiol.* 77, 498–504. doi: 10.1128/AEM.01661-10
- Barak, J. D., Liang, A., and Narm, K. E. (2008). Differential attachment to and subsequent contamination of agricultural crops by *Salmonella enterica*. *Appl. Environ. Microbiol.* 74, 5568–5570. doi: 10.1128/AEM.01077-08
- Berger, C. N., Shaw, R. K., Brown, D. J., Mather, H., Clare, S., Dougan, G., et al. (2009). Interaction of *Salmonella enterica* with basil and other salad leaves. *ISME J.* 3, 261–265. doi: 10.1038/ismej.2008.95
- Bock, C. H., Chiang, K.-S., and Del Ponte, E. M. (2022). Plant disease severity estimated visually: a century of research, best practices, and opportunities for improving methods and practices to maximize accuracy. *Trop. Plant. Pathol.* 47, 25–42. doi: 10.1007/s40858-021-00439-z
- Boureau, T., Routtu, J., Roine, E., Taira, S., and Romantschuk, M. (2002). Localization of *hrpA*-induced *Pseudomonas syringae* pv. *tomato* DC3000 in infected tomato leaves. *Mol. Plant Pathol.* 3, 451–460. doi: 10.1046/j.1364-3703.2002.00139.x
- Chahar, M., Kroupitski, Y., Gollop, R., Belausov, E., Melotto, M., and Sela-Saldinger, S. (2021). Determination of *Salmonella enterica* leaf internalization varies substantially according to the method and conditions used to assess bacterial localization. *Front. Microbiol.* 12:622068. doi: 10.3389/fmicb.2021.622068
- Cowles, K. N., Block, A. K., and Barak, J. D. (2022). *Xanthomonas hortorum* pv. *Gardneri* TAL effector AvrHah1 is necessary and sufficient for increased persistence of *Salmonella enterica* on tomato leaves. *Sci. Rep.* 12:7313. doi: 10.1038/s41598-022-11456-6
- Cowles, K. N., Groves, R. L., and Barak, J. D. (2018). Leafhopper-induced activation of the jasmonic acid response benefits *Salmonella enterica* in a flagellum-dependent manner. *Front. Microbiol.* 9:1987. doi: 10.3389/fmicb.2018.01987
- Daszkowska-Golec, A., and Szarejko, I. (2013). Open or close the gate – stomata action under the control of phytohormones in drought stress conditions. *Front. Plant Sci.* 4:138. doi: 10.3389/fpls.2013.00138
- Dixon, M. H., Cowles, K. N., Zaacks, S. C., Marciniak, I. N., and Barak, J. D. (2022). *Xanthomonas* infection transforms the Apoplast into an accessible and habitable niche for *Salmonella enterica*. *Appl. Environ. Microbiol.* 88:e0133022. doi: 10.1128/aem.01330-22
- Doan, H. K., Ngassam, V. N., Gilmore, S. F., Tecon, R., Parikh, A. N., and Leveau, J. H. J. (2020). Topography-driven shape, spread, and retention of leaf surface water impacts microbial dispersion and activity in the Phyllosphere. *Phytobiomes J.* 4, 268–280. doi: 10.1094/PBIOMES-01-20-0006-R
- Doehlemann, G., Wahl, R., Horst, R. J., Voll, L. M., Usadel, B., Poree, F., et al. (2008). Reprogramming a maize plant: transcriptional and metabolic changes induced by the fungal biotroph *Ustilago maydis*. *Plant J.* 56, 181–195. doi: 10.1111/j.1365-313X.2008.03590.x
- Fahrig, L. (2003). Effects of habitat fragmentation on biodiversity. *Annu. Rev. Ecol. Syst.* 34, 487–515. doi: 10.1146/annurev.ecolsys.34.011802.132419
- Freeman, B. C., and Beattie, G. A. (2009). Bacterial growth restriction during host resistance to *Pseudomonas syringae* is associated with leaf water loss and localized cessation of vascular activity in *Arabidopsis thaliana*. *Mol. Plant-Microbe Interact.* 22, 857–867. doi: 10.1094/MPMI-22-7-0857
- Gao, M., Xiong, C., Gao, C., Tsui, C. K. M., Wang, M.-M., Zhou, X., et al. (2021). Disease-induced changes in plant microbiome assembly and functional adaptation. *Microbiome* 9:187. doi: 10.1186/s40168-021-01138-2
- Geisler, M., Nadeau, J., and Sack, F. D. (2000). Oriented asymmetric divisions that generate the stomatal spacing pattern in *Arabidopsis* are disrupted by the too many mouths mutation. *Plant Cell* 12, 2075–2086. doi: 10.1105/tpc.12.11.2075
- Gentzel, I., Giese, L., Ekanayake, G., Mikhail, K., Zhao, W., Cocuron, J. C., et al. (2022). Dynamic nutrient acquisition from a hydrated apoplast supports biotrophic proliferation of a bacterial pathogen of maize. *Cell Host Microbe* 30:e4, 502–517.e4. doi: 10.1016/j.chom.2022.03.017
- Ginnan, N. A., Dang, T., Bodaghi, S., Ruegger, P. M., McCollum, G., England, G., et al. (2020). Disease-induced microbial shifts in Citrus indicate microbiome-derived responses to Huanglongbing across the disease severity Spectrum. *Phytobiomes J.* 4, 375–387. doi: 10.1094/PBIOMES-04-20-0027-R
- Gohlke, J., and Deeken, R. (2014). Plant responses to *agrobacterium tumefaciens* and crown gall development. *Front. Plant Sci.* 5:155. doi: 10.3389/fpls.2014.00155
- Golberg, D., Kroupitski, Y., Belausov, E., Pinto, R., and Sela, S. (2011). *Salmonella* Typhimurium internalization is variable in leafy vegetables and fresh herbs. *Int. J. Food Microbiol.* 145, 250–257. doi: 10.1016/j.ijfoodmicro.2010.12.031
- Griffiths, S. M., Galambao, M., Rowntree, J., Goodhead, I., Hall, J., O'Brien, D., et al. (2020). Complex associations between cross-kingdom microbial endophytes and host genotype in ash dieback disease dynamics. *J. Ecol.* 108, 291–309. doi: 10.1111/1365-2745.13302

Conflict of interest

The authors declare that the research was conducted in the absence of any commercial or financial relationships that could be construed as a potential conflict of interest.

Generative AI statement

The authors declare that no Gen AI was used in the creation of this manuscript.

Publisher's note

All claims expressed in this article are solely those of the authors and do not necessarily represent those of their affiliated organizations, or those of the publisher, the editors and the reviewers. Any product that may be evaluated in this article, or claim that may be made by its manufacturer, is not guaranteed or endorsed by the publisher.

Supplementary material

The Supplementary material for this article can be found online at: <https://www.frontiersin.org/articles/10.3389/fmicb.2025.1546411/full#supplementary-material>

- Haefele, D. M., and Lindow, S. E. (1987). Flagellar motility confers epiphytic fitness advantages upon *Pseudomonas syringae*. *Appl. Environ. Microbiol.* 53, 2528–2533. doi: 10.1128/aem.53.10.2528-2533.1987
- Harrod, V. L., Groves, R. L., Guillemette, E. G., and Barak, J. D. (2022). *Salmonella enterica* changes *macrosteles quadrilineatus* feeding behaviors resulting in altered *S. enterica* distribution on leaves and increased populations. *Sci. Rep.* 12:8544. doi: 10.1038/s41598-022-11750-3
- Hood, R. D., Singh, P., Hsu, F., Guvener, T., Carl, M. A., Trinidad, R. R., et al. (2010). A type VI secretion system of *Pseudomonas aeruginosa* targets a toxin to bacteria. *Cell Host Microbe* 7, 25–37. doi: 10.1016/j.chom.2009.12.007
- Hu, Y., Ding, Y., Cai, B., Qin, X., Wu, J., Yuan, M., et al. (2022). Bacterial effectors manipulate plant abscisic acid signaling for creation of an aqueous apoplast. *Cell Host Microbe* 30, 518–529.e6. doi: 10.1016/j.chom.2022.02.002
- Hu, Q., Tan, L., Gu, S., Xiao, Y., Xiong, X., Zeng, W.-a., et al. (2020). Network analysis infers the wilt pathogen invasion associated with non-detrimental bacteria. *NPJ Biofilms Microbiomes* 6:8. doi: 10.1038/s41522-020-0117-2
- Huang, F., Ling, J., Zhu, C., Cheng, B., Song, X., and Peng, A. (2023). Canker disease intensifies cross-kingdom microbial interactions in the endophytic microbiota of Citrus Phyllosphere. *Phytobiomes J.* 7, 365–374. doi: 10.1094/PBIOMES-11-22-0091-R
- Jones, J., Stall, R., and Bouzar, H. (1998). Diversity among xanthomonads pathogenic on pepper and tomato. *Annu. Rev. Phytopathol.* 36, 41–58. doi: 10.1146/annurev.phyto.36.1.41
- Kessens, R., Sorensen, N., and Kabbage, M. (2018). An inhibitor of apoptosis (SflAP) interacts with SQUAMOSA promoter-binding protein (SBP) transcription factors that exhibit pro-cell death characteristics. *Plant Direct* 2:e00081. doi: 10.1002/pld3.81
- Kinkel, L. L. (1997). Microbial population dynamics on leaves. *Annu. Rev. Phytopathol.* 35, 327–347. doi: 10.1146/annurev.phyto.35.1.327
- Kinkel, L. L., Wilson, M., and Lindow, S. E. (2000). Plant species and plant incubation conditions influence variability in epiphytic bacterial population size. *Microb. Ecol.* 39, 1–11. doi: 10.1007/s002489900182
- Knief, C., Ramette, A., Frances, L., Alonso-Blanco, C., and Vorholt, J. A. (2010). Site and plant species are important determinants of the *Methylobacterium* community composition in the plant phyllosphere. *ISME J.* 4, 719–728. doi: 10.1038/ismej.2010.9
- Kraus, C. M., Mazo-Molina, C., Smart, C. D., and Martin, G. B. (2017). *Pseudomonas syringae* pv. *tomato* strains from New York exhibit virulence attributes intermediate between typical race 0 and race 1 strains. *Plant Dis.* 101, 1442–1448. doi: 10.1094/PDIS-03-17-0330-RE
- Kwan, G., Charkowski, A. O., and Barak, J. D. (2013). *Salmonella enterica* suppresses *Pectobacterium carotovorum* subsp. *carotovorum* population and soft rot progression by acidifying the microaerophilic environment. *MBio* 4, e00557–e00512. doi: 10.1128/mBio.00557-12
- Kwan, G., Pisithkul, T., Amador-Noguez, D., and Barak, J. (2015). De novo amino acid biosynthesis contributes to *Salmonella enterica* growth in alfalfa seedling exudates. *Appl. Environ. Microbiol.* 81, 861–873. doi: 10.1128/AEM.02985-14
- Leveau, J. H., and Lindow, S. E. (2001). Appetite of an epiphyte: quantitative monitoring of bacterial sugar consumption in the phyllosphere. *Proc. Natl. Acad. Sci. USA* 98, 3446–3453. doi: 10.1073/pnas.061629598
- Li, P.-D., Zhu, Z.-R., Zhang, Y., Xu, J., Wang, H., Wang, Z., et al. (2022). The phyllosphere microbiome shifts toward combating melanose pathogen. *Microbiome* 10:56. doi: 10.1186/s40168-022-01234-x
- Lindow, S. E., Andersen, G., and Beattie, G. A. (1993). Characteristics of insertional mutants of *Pseudomonas syringae* with reduced epiphytic fitness. *Appl. Environ. Microbiol.* 59, 1593–1601. doi: 10.1128/aem.59.5.1593-1601.1993
- Manos, J. (2022). The human microbiome in disease and pathology. *APMIS* 130, 690–705. doi: 10.1111/apm.13225
- Mazo-Molina, C., Mainiero, S., Hind, S. R., Kraus, C. M., Vachev, M., Maviane-Macia, E., et al. (2019). The Ptr1 locus of *Solanum lycopersicoides* confers resistance to race 1 strains of *Pseudomonas syringae* pv. *tomato* and to *Ralstonia pseudosolanacearum* by recognizing the type III effectors AvrRpt2 and RipBN. *Mol. Plant-Microbe Interact.* 32, 949–960. doi: 10.1094/MPMI-01-19-0018-R
- McIntyre, K. E., Bush, D. R., and Argueso, C. T. (2021). Cytokinin regulation of source-sink relationships in plant-pathogen interactions. *Front. Plant Sci.* 12:677585. doi: 10.3389/fpls.2021.677585
- Melotto, M., Underwood, W., and He, S. Y. (2008). Role of stomata in plant innate immunity and foliar bacterial diseases. *Annu. Rev. Phytopathol.* 46, 101–122. doi: 10.1146/annurev.phyto.121107.104959
- Melotto, M., Underwood, W., Koczan, J., Nomura, K., and He, S. Y. (2006). Plant stomata function in innate immunity against bacterial invasion. *Cell* 126, 969–980. doi: 10.1016/j.cell.2006.06.054
- Melotto, M., Zhang, L., Oblessuc, P. R., and He, S. Y. (2017). Stomatal defense a decade later. *Plant Physiol.* 174, 561–571. doi: 10.1104/pp.16.01853
- Miller, W. G., Leveau, J. H., and Lindow, S. E. (2000). Improved *gfp* and *inaZ* broad-host-range promoter-probe vectors. *Mol. Plant-Microbe Interact.* 13, 1243–1250. doi: 10.1094/MPMI.2000.13.11.1243
- Monier, J. M., and Lindow, S. E. (2003). Differential survival of solitary and aggregated bacterial cells promotes aggregate formation on leaf surfaces. *Proc. Natl. Acad. Sci. USA* 100, 15977–15982. doi: 10.1073/pnas.2436560100
- Monier, J. M., and Lindow, S. E. (2004). Frequency, size, and localization of bacterial aggregates on bean leaf surfaces. *Appl. Environ. Microbiol.* 70, 346–355. doi: 10.1128/AEM.70.1.346-355.2004
- Nir, I., Shohat, H., Panizel, I., Olszewski, N., Aharoni, A., and Weiss, D. (2017). The tomato DELLA protein PROCERA acts in guard cells to promote stomatal closure. *Plant Cell* 29, 3186–3197. doi: 10.1105/tpc.17.00542
- Nix, S., Burpee, L. L., and Buck, J. W. (2009). Responses of 2 epiphytic yeasts to foliar infection by *Rhizoctonia solani* or mechanical wounding on the phylloplane of tall fescue. *Can. J. Microbiol.* 55, 1160–1165. doi: 10.1139/W09-072
- Osdaghi, E., Jones, J. B., Sharma, A., Goss, E. M., Abrahamian, P., Newberry, E. A., et al. (2021). A centenary for bacterial spot of tomato and pepper. *Mol. Plant Pathol.* 22, 1500–1519. doi: 10.1111/mpp.13125
- Potnis, N., Colee, J., Jones, J. B., and Barak, J. D. (2015). Plant pathogen-induced water-soaking promotes *Salmonella enterica* growth on tomato leaves. *Appl. Environ. Microbiol.* 81, 8126–8134. doi: 10.1128/AEM.01926-15
- Potnis, N., Soto-Arias, J. P., Cowles, K. N., van Bruggen, A. H., Jones, J. B., and Barak, J. D. (2014). *Xanthomonas perforans* colonization influences *Salmonella enterica* in the tomato phyllosphere. *Appl. Environ. Microbiol.* 80, 3173–3180. doi: 10.1128/AEM.00345-14
- Pride, L., Vallad, G., and Agehara, S. (2020). How to measure leaf disease damage using image analysis in ImageJ: HSI382, 9/2020. *EDIS* 2020. doi: 10.32473/edis-hsi382-2020 [Epub ahead of print].
- Remus-Emsermann, M. N., and Leveau, J. H. (2010). Linking environmental heterogeneity and reproductive success at single-cell resolution. *ISME J.* 4, 215–222. doi: 10.1038/ismej.2009.110
- Remus-Emsermann, M. N., Tecon, R., Kowalchuk, G. A., and Leveau, J. H. (2012). Variation in local carrying capacity and the individual fate of bacterial colonizers in the phyllosphere. *ISME J.* 6, 756–765. doi: 10.1038/ismej.2011.209
- Rodenburg, S. Y. A., Seidl, M. F., Judelson, H. S., Vu, A. L., Govers, F., and de Ridder, D. (2019). Metabolic model of *Thephytophthora infestans*-tomato interaction reveals metabolic switches during host colonization. *mBio* 10:e00454-19. doi: 10.1128/mBio.00454-19
- Roussin-Léveillé, C., Lajeunesse, G., St-Amand, M., Veerapen, V. P., Silva-Martins, G., Nomura, K., et al. (2022). Evolutionarily conserved bacterial effectors hijack abscisic acid signaling to induce an aqueous environment in the apoplast. *Cell Host Microbe* 30, 489–501.e4. doi: 10.1016/j.chom.2022.02.006
- Roussin-Leveille, C., Mackey, D., Ekanayake, G., Gohmann, R., and Moffett, P. (2024). Extracellular niche establishment by plant pathogens. *Nat. Rev. Microbiol.* 22, 360–372. doi: 10.1038/s41579-023-00999-8
- Rufian, J. S., Macho, A. P., Corry, D. S., Mansfield, J. W., Ruiz-Albert, J., Arnold, D. L., et al. (2018). Confocal microscopy reveals in planta dynamic interactions between pathogenic, avirulent and non-pathogenic *Pseudomonas syringae* strains. *Mol. Plant Pathol.* 19, 537–551. doi: 10.1111/mpp.12539
- Schlechter, R. O., Miebach, M., and Remus-Emsermann, M. N. (2019). Driving factors of epiphytic bacterial communities: a review. *J. Adv. Res.* 19, 57–65. doi: 10.1016/j.jare.2019.03.003
- Schneider, C. A., Rasband, W. S., and Eliceiri, K. W. (2012). NIH image to ImageJ: 25 years of image analysis. *Nat. Methods* 9, 671–675. doi: 10.1038/nmeth.2089
- Soylu, S., Brown, I., and Mansfield, J. W. (2005). Cellular reactions in Arabidopsis following challenge by strains of *Pseudomonas syringae*: from basal resistance to compatibility. *Physiol. Mol. Plant Pathol.* 66, 232–243. doi: 10.1016/j.pmp.2005.08.005
- Stall, R. E., and Hall, C. B. (1984). Chlorosis and ethylene production in pepper leaves infected by *Xanthomonas campestris* pv. *vesicatoria*. *Physiol. Biochem.* 74, 373–375. doi: 10.1094/Phyto-74-373
- Timilsina, S., Potnis, N., Newberry, E. A., Liyanapathirana, P., Iruegas-Bocardo, F., White, F. F., et al. (2020). *Xanthomonas* diversity, virulence and plant-pathogen interactions. *Nat. Rev. Microbiol.* 18, 415–427. doi: 10.1038/s41579-020-0361-8
- van der Walt, S., Schonberger, J. L., Nunez-Iglesias, J., Boulogne, F., Warner, J. D., Yager, N., et al. (2014). scikit-image: image processing in Python. *PeerJ* 2:e453. doi: 10.7717/peerj.453
- Ward, J. L., Forcat, S., Beckmann, M., Bennett, M., Miller, S. J., Baker, J. M., et al. (2010). The metabolic transition during disease following infection of *Arabidopsis thaliana* by *Pseudomonas syringae* pv. *tomato*. *Plant J.* 63, 443–457. doi: 10.1111/j.1365-3113.2010.04254.x
- Wells, J. M., and Butterfield, J. E. (1997). *Salmonella* contamination associated with bacterial soft rot of fresh fruits and vegetables in the marketplace. *Plant Dis.* 81, 867–872. doi: 10.1094/PDIS.1997.81.8.867
- Wilson, M., and Lindow, S. E. (1994a). Coexistence among epiphytic bacterial populations mediated through nutritional resource partitioning. *Appl. Environ. Microbiol.* 60, 4468–4477. doi: 10.1128/aem.60.12.4468-4477.1994
- Wilson, M., and Lindow, S. E. (1994b). Inoculum density-dependent mortality and colonization of the Phyllosphere by *Pseudomonas syringae*. *Appl. Environ. Microbiol.* 60, 2232–2237. doi: 10.1128/aem.60.7.2232-2237.1994
- Wilson, M., and Lindow, S. E. (1995). Enhanced epiphytic coexistence of near-isogenic salicylate-catabolizing and non-salicylate-catabolizing *Pseudomonas putida* strains after exogenous salicylate application. *Appl. Environ. Microbiol.* 61, 1073–1076. doi: 10.1128/aem.61.3.1073-1076.1995

Woody, S. T., Ives, A. R., Nordheim, E. V., and Andrews, J. H. (2007). Dispersal, density dependence, and population dynamics of a fungal microbe on leaf surfaces. *Ecology* 88, 1513–1524. doi: 10.1890/05-2026

Xian, L., Yu, G., Wei, Y., Rufian, J. S., Li, Y., Zhuang, H., et al. (2020). A bacterial effector protein hijacks plant metabolism to support pathogen nutrition. *Cell Host Microbe* 28:e7, 548–557.e7. doi: 10.1016/j.chom.2020.07.003

Xin, X.-F., Nomura, K., Aung, K., Velásquez, A. C., Yao, J., Boutrot, F., et al. (2016). Bacteria establish an aqueous living space in plants crucial for virulence. *Nature* 539, 524–529. doi: 10.1038/nature20166

Yang, F., Zhang, J., Zhang, H., Ji, G., Zeng, L., Li, Y., et al. (2020). Bacterial blight induced shifts in endophytic microbiome of Rice leaves and the enrichment of specific bacterial strains with pathogen antagonism. *Front. Plant Sci.* 11:963. doi: 10.3389/fpls.2020.00963